World Journal of Urology (2020) 38:2513–2521
https://doi.org/10.1007/s00345-019-03066-1

ORIGINAL ARTICLE

Simultaneous whole-body PET/MRI with integrated multiparametric MRI for primary staging of high-risk prostate cancer

Sascha Kaufmann[1] · Stephan Kruck[2] · Sergios Gatidis[1] · Tobias Hepp[1] · Wolfgang M. Thaiss[1] · Jörg Hennenlotter[2] · Johannes Schwenck[3] · Marcus Scharpf[4] · Konstantin Nikolaou[1] · Arnulf Stenzl[2] · Gerald Reischl[5] · Christian la Fougère[3,6,7] · Jens Bedke[2,7]

Received: 22 October 2019 / Accepted: 21 December 2019 / Published online: 6 January 2020

Abstract

Purpose Whole-body positron emission tomography/magnetic resonance imaging (wbPET/MRI) is a promising diagnostic tool of recurrent prostate cancer (PC), but its role in primary staging of high-risk PC (hrPC) is not well defined. Thus, the aim was to compare the diagnostic accuracy for T-staging of PET-blinded reading (PBR) and PET/MRI.

Methods In this prospective study, hrPC patients scheduled to radical prostatectomy (RPx) with extended lymphadenectomy (eLND) were staged with wbPET/MRI and either ^{68}Ga-PSMA-11 or ^{11}C-choline including simultaneous multiparametric MRI (mpMRI). Images were assessed in two sessions, first as PBR (mpMRI and wbMRI) and second as wbPET/MRI. Prostate Imaging Reporting and Data System criteria (PIRADS v2) were used for T-staging. Results were correlated with the exact anatomical localization and extension as defined by histopathology. Diagnostic accuracy of cTNM stage according to PBR was compared to pathological pTNM stage as reference standard.

Results Thirty-four patients underwent wbPET/MRI of ^{68}Ga-PSMA-11 ($n=17$) or ^{11}C-choline ($n=17$). Twenty-four patients meeting the inclusion criteria of localized disease ± nodal disease based on imaging results underwent RPx and eLND, whereas ten patients were excluded from analysis due to metastatic disease. T-stage was best defined by mpMRI with underestimation of tumor lesion size by PET for both tracers. N-stage yielded a per patient sensitivity/specificity comparable to PBR.

Conclusion MpMRI is the primary modality for T-staging in hrPC as PET underestimated T-stage in direct comparison to final pathology. In this selected study, cohort MRI shows no inferiority compared to wbPET/MRI considering N-staging.

Keywords Prostate cancer · PET · PSMA · MRI · Choline

Introduction

Prostate cancer (PC) represents the most common non-cutaneous cancer in men in North America and Europe and is a leading cause of cancer-related death worldwide [1]. More than 15% of men with PC are confronted with high-risk

Electronic supplementary material The online version of this article (https://doi.org/10.1007/s00345-019-03066-1) contains supplementary material, which is available to authorized users.

✉ Wolfgang M. Thaiss
wolfgang.thaiss@med.uni-tuebingen.de

[1] Department of Diagnostic and Interventional Radiology, University Hospital Tübingen, Hoppe-Seyler-Str. 3, 72076 Tübingen, Germany

[2] Department of Urology, University Hospital Tuebingen, Hoppe-Seyler-Str. 3, 72076 Tübingen, Germany

[3] Department of Nuclear Medicine and Clinical Molecular Imaging, University Hospital Tübingen, Otfried-Müller-Straße 14, 72076 Tübingen, Germany

[4] Institute of Pathology, Eberhard-Karls-University, Liebermeisterstraße 8, 72076 Tübingen, Germany

[5] Department of Preclinical Imaging and Radiopharmacy, University Hospital Tübingen, Röntgenweg 13, 72076 Tübingen, Germany

[6] Cluster of Excellence iFIT (EXC 2180) "Image Guided and Functionally Instructed Tumor Therapies", University of Tübingen, Tübingen, Germany

[7] German Cancer Consortium (DKTK), Partner Site Tübingen, Germany

PC (hrPC), which is defined by a prostate-specific antigen (PSA) concentration > 20 ng/mL, a Gleason score ≥ 8, or a American Joint Commission on Cancer (AJCC) tumour (T) category ≥ 2c [2, 3]. HrPC harbours a higher risk for locally advanced disease, extracapsular extension (ECE), seminal vesicle extension (SVI), lymph-node metastases (LNM), and bone metastases [4]; therefore, an additional whole-body staging prior to therapy initiation should be performed [5]. Recent reports suggest that PC with minimal lymph-node (LN) involvement, called oligo nodal disease (OND), can be cured by extended lymph-node dissection (eLND) when RP is performed as initial therapy [6–8].

Irrespective of the treatment decision (surgical versus radiation-based), developments in treatment require a reliable and accurate staging modality for patient selection. Current guidelines recommend the use of PET/CT, and MRI for evaluation of LNM in patients with high-risk disease [9]. Local staging with multiparametric MRI (mpMRI) has become widely available and is used to assess the local extent of prostate tumors. The traditional imaging criteria for the differentiation between benign lymph nodes (LN) from LNM based on nodal size and irregular shape show low sensitivity for smaller LNMs [10]. To overcome these limitations, hybrid imaging has been introduced for PC imaging [11, 12]. First retrospective studies were performed comparing radiolabelled choline derivatives and a prostate-specific-membrane-antigen (PSMA) targeting tracer [13], and could reveal a significant increase in the detection rate of LNM by ^{68}Ga-PSMA-PET/CT. Therefore, in several countries, PSMA-specific tracers displaced radiolabelled choline in PET imaging of PC. Nevertheless, most reports on PSMA-PET/CT and PSMA-PET/MRI are retrospective studies or investigating a small sample sizes and patient cohorts with heterogeneous characteristics [14, 15]. Due to limited spatial resolution of PET and the lack of anatomic detail within the prostate, neither PSMA-based nor choline-based-PET/CT has outperformed MRI, which still remains the gold standard for local staging of prostate cancer [12]. The advantages of combining PET and MRI imaging have been elucidated in several publications in the last years. The main limitation of currently available PET/MRI data is the lack of histopathological confirmation, especially concerning the LN status, while the majority of the published data focus on recurrent prostate cancer, which is currently the main indication for the use of PSMA-based PET imaging [16].

Whether local staging needs the additional functional information of PET imaging, or if this functional information is only needed for extraprostatic disease is of debate [17]. Thus, the aim of this prospective study was to evaluate the diagnostic performance of combined PET/MRI using ^{68}Ga-PSMA-11 or ^{11}C-choline for local (T-stage) and lymph-node staging (N-stage) of patients with hrPC, validated by histopathology.

Materials and methods

This prospective study was performed in agreement with the Declaration of Helsinki and with approval from the local institutional review board (241/2012MPG23). All patients were included in an interdisciplinary institutional tumor board. All patients gave written informed consent for the participation in this study. Inclusion criteria included: newly diagnosed hrPC confirmed by histopathology and scheduled for RP. Exclusion criteria were: suspicion of bone metastasis due to bone pain or marked increase of alkaline phosphatase (ALP), acute inflammation, contraindications for MRI, known claustrophobia, or renal function impairment. The inclusion criteria are summarized in Supplementary Table 1. Imaging was performed not earlier than 8 weeks after prostate biopsy to avoid relevant signal alterations due to biopsy. In case of OND (N1) and ≤ 5 nodal metastases without bone metastasis, patients were treated with curative intent. The extended LND (eLND) included a standardized template of fossa obturatoria and arteria iliaca externa, interna, and communis.

PET/MRI including multiparametric MRI

Imaging was performed using an integrated whole-body PET/MRI system (Siemens Biograph mMR, Siemens Healthineers, Erlangen, Germany). PET acquisition was initiated 60 min after injection of 620 ± 30 MBq ^{11}C-choline/60 min after injection of 190 ± 40 MBq ^{68}Ga-PSMA-11 respectively. Synthesis of both tracers is described elsewhere [15]. All patients were asked to void urine directly before the start of the examination, Erlangen, Germany. The PET/MR protocol included a whole-body scan with 4 min PET acquisition per bed position together with a T2w-haste sequence in axial and coronal orientation, a coronal STIR sequence, diffusion-weighted imaging, and an attenuation correction scan. This WB scan was followed by a dedicated PI-RADS v2 compliant local mpMRI protocol of the pelvis including a T2w TSE sequence in three orientations, diffusion-weighted imaging and dynamic contrast enhanced imaging, accompanied by simultaneous PET acquisition of the pelvic regions. For the pelvic scan, the PET imaging was repeated over the pelvic region to ensure optimal alignment.

Image analysis

Four experienced readers, two nuclear medicine physicians and two radiologists, aware of the PC diagnosis but not of other clinical and histopathological findings, staged the tumor extension in the prostatic gland based on the PI-RADS v2.0 scheme in consensus. The size of detected

lesions was measured on axial T2w images. Each lesion was localized into the sector map diagram proposed by PI-RADS v2 [18]. In the next step, the same readers visually evaluated the wbMRI in a PET-blinded reading procedure. In the last step, the additional value of PET in PET/MRI was evaluated. Every focal radiotracer uptake, which was not consistent to the physiological distribution of the individual tracer, was considered suspicious for malignancy and defined as PET positive. Focal uptake in the prostate beyond that of adjacent background was considered to be malignant. Standardized uptake values (SUVmean) of the primary tumor were quantified using a 50% volume-of-interest (VOI) isocontour in PET/MRI. Lymph-node metastases were considered pathological on morphological imaging (MRI) when the short-axis diameter exceeded 1 cm. In PET, lymph nodes were considered metastatic if a clearly increased focal tracer uptake was observed visually together with a morphologic correlate in MRI. The readers determined TNM staging based on PET-blinded MRI reading, as well as based on PET/MRI. Histopathology was consulted after the reading. In patient-based analysis, the detection rate was defined as the ability to detect at least one pathological finding in each individual subject.

Histopathology analysis and staging

All RP specimens were processed as whole-mount section pathology with a slice thickness of 3 mm with angulation based on PET/MRI acquisition. The presence and location of cancer foci, high-grade prostatic intraepithelial neoplasia, prostatitis, BPH, capsular status, and seminal vesicle invasion were determined. For each tumor focus, GS was assigned as a combination of primary, secondary, and tertiary (when applicable) Gleason grade. LNs with a diameter of >5 mm were sliced longitudinally in three parts along the greatest dimension. All prostates and dissected lymph nodes were reviewed by one experienced uropathologist. Staging was done according to the 2009 TNM classification for staging of prostate cancer based on cT, GS, and PSA [19].

Statistical analysis

Descriptive statistics were used to characterise the patient population. Continuous variables are presented as median and interquartile range (IQR) and differences between groups were assessed by the Kruskal–Wallis test. Categorical variables were tested with the Chi-square test or Fisher's exact test. Multiple method comparison was tested with the extended Bland–Altman plot with comparison of the single methods against the reference method. All statistical analyses were completed using SPSS, version 22. For all statistical comparisons, significance was considered as $p<0.05$.

Results

From January 2013 to June 2016, 34 patients with histopathological confirmed, non-treated hrPC were included prospectively (see Fig. 1). All patients underwent wbPET/MRI including mpMRI with either ^{68}Ga-PSMA-11 ($n=17$) and ^{11}C-choline ($n=17$). Median age was 67.0 years [IQR (interquartile range) 46.0–72.0 years]; median PSA was 16.3 ng/mL (IQR 8.3–46.0). 24/34 patients underwent radical prostatectomy within a median of 7 days (range 1–12) after the PET/MRI study with extended lymph-node dissection (eLND). Surgery was also performed as part of a multimodal treatment, even when OND was detected by imaging. The local tumor board reassessed the initial therapeutic approach to evaluate its impact on the therapeutic management. 10/34 patients underwent a non-surgical treatment due to extended, non-regional lymph-node involvement (defined as PET positive and morphological suspect; $n=6$; four out of these in choline and two in PSMA-PET) and/or bone metastasis ($n=5$; four out of these in choline and one in PSMA-PET) detected in PET/MRI. All patients undergoing RP showed a GS $\geq 4+4$ and a significant tumor volume of >2.5 mL. Table 1 lists the baseline and the pathological characteristics of patients in all patients who underwent surgery.

T-staging

In all 24 patients treated with RP and eLND, PET/MRI examinations were evaluated in consensus by the four blinded experienced readers based on mpMRI, whole-body MRI, and PET imaging. No changes related to prior biopsy (e.g., hyperintense signal in non-contrast enhanced T1w sequences) were present. The PC index lesions, defined as the dominant intraprostatic lesion, could be detected in all cases by mpMRI as well as by PET. In comparison to the pathohistological gold standard, both modalities found the main tumor mass in the location of the whole-mount section.

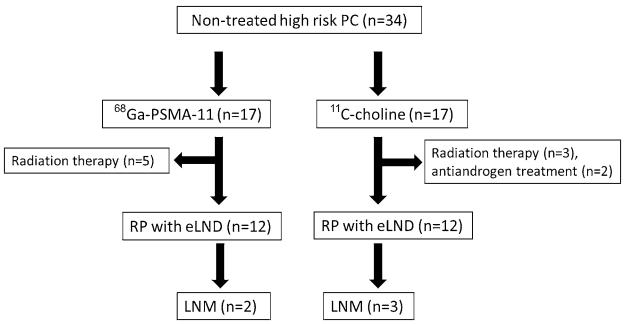

Fig. 1 Flowchart: 34 patients with histopathological confirmed, non-treated high-risk PC were included prospectively

Table 1 Baseline and pathological characteristics of all surgical-treated patients meeting the inclusion criteria of localized disease ± oligo nodal disease based on imaging results, and underwent radical prostatectomy and extended lymph-node dissection (undergoing PET/MRI with either ^{11}C-choline, ^{68}Ga-PSMA-11)

Tracer	Pathological TNM	Gleason biopsy	Gleason RP	LNM/ removed LN	N + based on PET/ MRI	N + PET-blinded	PSA (ng/mL)	PI-RADS	PET false negative	PET false positive	mpMRI size	PET size	Pathohistological size
^{11}C-choline	pT3b, pN0	4 + 5 = 9	4 + 4 = 8	0/24	0	0	10.5	5	0	0	3.6	1.8	3.6
^{11}C-choline	pT3a, pN1	4 + 5 = 9	4 + 4 = 8	1/26	0	0	6.7	4	1 (missed LNM)	0	1	1	1
^{11}C-choline	pT2c, pN0	4 + 5 = 9	4 + 4 = 8	0/22	0	0	6.6	4	0	0	1.4	1.4	1.4
^{11}C-choline	pT2c, pN0	4 + 4 = 8	4 + 4 = 8	0/24	0	0	7.5	4	0	0	1.1	1.1	1.1
^{11}C-choline	pT4, pN0	5 + 5 = 10	4 + 5 = 9	0/27	0	0	46.0	5	0	0	3	3	3
^{11}C-choline	pT3b, pN1	4 + 5 = 9	4 + 5 = 9	4/23	2	1	6.3	5	1 (underestimation of LNM)	0	2.4	1.9	2.4
^{11}C-choline	pT2c, pN0	4 + 5 = 9	4 + 4 = 8	0/25	0	0	13.0	5	0	0	2.1	1.6	2.1
^{11}C-choline	pT3a, pN0	4 + 4 = 8	4 + 4 = 8	0/22	0	0	25.0	5	0	0	3	2.4	3
^{11}C-choline	pT2c, pN1	4 + 4 = 8	4 + 4 = 8	1/51	0	0	17.1	4	1 (missed LNM)	0	1.4	1.4	1.4
^{11}C-choline	pT2c, pN0	4 + 4 = 8	4 + 4 = 8	0/51	0	0	16.7	5	0	0	1.6	1.2	1.6
^{11}C-choline	pT3a, pN0	4 + 5 = 9	4 + 4 = 8	0/33	0	0	11.0	5	0	0	1.5	1.5	1.5
^{11}C-choline	pT2c, pN0	4 + 5 = 9	4 + 5 = 9	0/39	0	0	7.8	5	0	0	1.7	1.7	1.7
^{68}Ga-PSMA-11	pT2c, pN0	4 + 4 = 8	4 + 4 = 8	0/21	0	0	20.1	5	0	0	2.8	1.9	2.8
^{68}Ga-PSMA-11	pT2c, pN0	4 + 4 = 8	4 + 4 = 8	0/24	0	0	17.0	4	0	0	1.3	1.3	1.3
^{68}Ga-PSMA-11	pT2b, pN0	4 + 4 = 8	4 + 4 = 8	0/26	0	0	8.3	5	0	0	1.6	1.6	1.6
^{68}Ga-PSMA-11	pT2c, pN0	4 + 4 = 8	4 + 4 = 8	0/25	0	0	8.9	5	0	0	1.6	1.6	1.6
^{68}Ga-PSMA-11	pT3b, pN1	4 + 5 = 9	4 + 5 = 9	2/37	1	1	12.3	5	1 (underestimation of LNM)	0	4.5	4.5	4.5
^{68}Ga-PSMA-11	pT3a, pN0	4 + 5 = 9	4 + 5 = 9	0/26	0	0	13.4	5	0	0	2.6	1.8	2.6
^{68}Ga-PSMA-11	pT3b, pN0	4 + 5 = 9	4 + 5 = 9	0/25	0	0	27.5	5	0	0	4.1	4.1	4.1
^{68}Ga-PSMA-11	pT2c, pN0	4 + 4 = 8	4 + 4 = 8	0/24	0	0	6.2	5	0	0	1.5	1.5	1.5
^{68}Ga-PSMA-11	pT3a, pN0	4 + 4 = 8	4 + 4 = 8	0/24	0	0	9.0	5	0	0	1.5	1.5	1.5

Table 1 (continued)

Tracer	Pathological TNM	Gleason biopsy	Gleason RP	LNM/ removed LN	N + based on PET/ MRI	N + PET-blinded	PSA (ng/mL)	PI-RADS	PET false negative	PET false positive	mpMRI size	PET size	Pathohistological size
^{68}Ga-PSMA-11	pT3a, pN0	4 + 4 = 8	4 + 4 = 8	0/21	0	0	10.4	5	0	0	1.5	1.5	1.5
^{68}Ga-PSMA-11	pT3b, pN1	4 + 4 = 8	4 + 4 = 8	1/20	0	0	14.0	5	1 (missed LNM)	0	1.8	1	1.8
^{68}Ga-PSMA-11	pT2c, pN0	4 + 4 = 8	4 + 4 = 8	0/22	0	0	29.0	5	0	0	2.8	1.6	2.8

LNM lymph-node metastasis, removed LN (number of surgical resected lymph nodes)

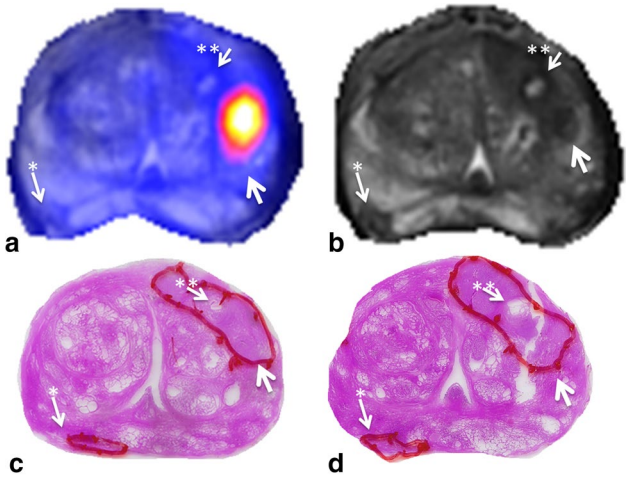

Fig. 2 66-year-old patient with a histologically proven high-risk PC in the left peripheral zone (Gleason 9) and a PSA level of 12.4 ng/mL. Fused PET/MRI (^{68}Ga-PSMA-11) transversal image (**a**) showed the underestimation of the local tumor extent by PET. T2-weighted transversal image (**b**) shows a lesion index lesion with strong hypointensity signal intensity (arrow **) and an additional tumor focus (arrow *) with no uptake in PSMA-PET. Whole-mount histology shows the tumor extent which correlates with extent in T2-weighted transversal image

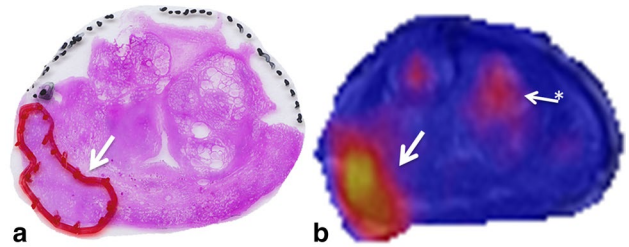

Fig. 3 70-year-old patient with a histologically proven high-risk PC in the right peripheral zone (Gleason 9) and a PSA level of 13.2 ng/mL. The whole-mount histology (**a**) shows the tumor extent which correlates good with extent in fused PET/MRI (^{11}C-choline) transversal image (**b**). Unspecific uptake in the transitional zone (**b**, arrow *)

When compared to the gold standard (histopathological tumor delineation), mpMRI was found to be more accurate (agreement on size in all cases) than PET imaging (agreement in 15/24 cases), as shown in Table 1. We found no significant differences between ^{11}C-choline and ^{68}Ga-PSMA-11 for local tumor detection. Both PET with ^{11}C-choline, as well as with ^{68}Ga-PSMA-11, underestimated the local tumor extent in comparison to mpMRI as well as histopathology (see Figs. 2, 3). Seminal vesicle invasion (pT3b) was detected in 6/24 patients (25%). MpMRI detected seminal vesicle invasion correctly in all cases, whereas PET did not show an increased focal uptake at this localization (T3b status was missed in six cases; three cases undergoing PSMA/

choline). Method comparison against the gold standard histology for T-staging resulted in a mean size difference for MRI of 0.2 ± 1.4% with a slight overestimation and for PET of − 12.1 ± 17.2% with an underestimation of size.

Lymph-node staging

662 LNs were resected with 9 harboring metastases (1%) in 5 of 24 patients (21%). A median of 25 (range 20–51) lymph nodes was removed during eLND. Of these five patients, two patients had undergone PET with ^{68}Ga-PSMA-11 and three patients had undergone PET with ^{11}C-choline. The PET/MRI scans identified 2/5 patients (one in PSMA-PET; one in choline PET) as LN positive (true positive). Both patients identified as nodal positive showed suspicious LN in MRI, whereas patients with PET-negative LN also showed no pathological enlargement or architectural signs of metastasis (see Fig. 4). The calculated per patient sensitivity, specificity, positive predictive value, negative predictive value, and accuracy were 50/100/100/90.9/90.9% for nodal staging by ^{68}Ga-PSMA-11-PET/MR. The calculated per patient sensitivity, specificity, positive predictive value, negative predictive value, and accuracy were 33.3/100/100/81.8/83.3% for nodal staging by ^{11}C-choline PET/MR.

Additional results can be found in the Supplementary Material.

Discussion

Currently, the optimal strategy for primary staging in patients with high-risk PC, including local tumor extension as well as lymph-node staging, is still under debate. Some years ago, choline tracers were the most used and studied tracers in prostate cancer. However, the sensitivity of choline PET/CT in the detection of lymph-node metastases in primary staging was reported to be relatively low, even in patients with high PSA values and high-risk Gleason scores [17]. The introduction of a ^{68}Ga-labeled PSMA-specific radiopharmaceutical promises a significant improvement in prostate cancer staging, but prospective studies evaluating the role for primary staging of hrPC are still lacking.

In the current prospective study, we reported the first histopathological confirmed matched pairs study in high-risk prostate cancer, comparing wbPET/MRI with integrated mpMRI with ^{11}C-choline or ^{68}Ga-PSMA-11 in terms of primary PC detection and assessment of tumor extent as well as lymph-node detection.

Our study yields several important findings. In particular, we observed similar overall PC detection between mpMRI and PET/MRI with ^{11}C-choline or ^{68}Ga-PSMA-11, while mpMRI showed a better precision concerning the

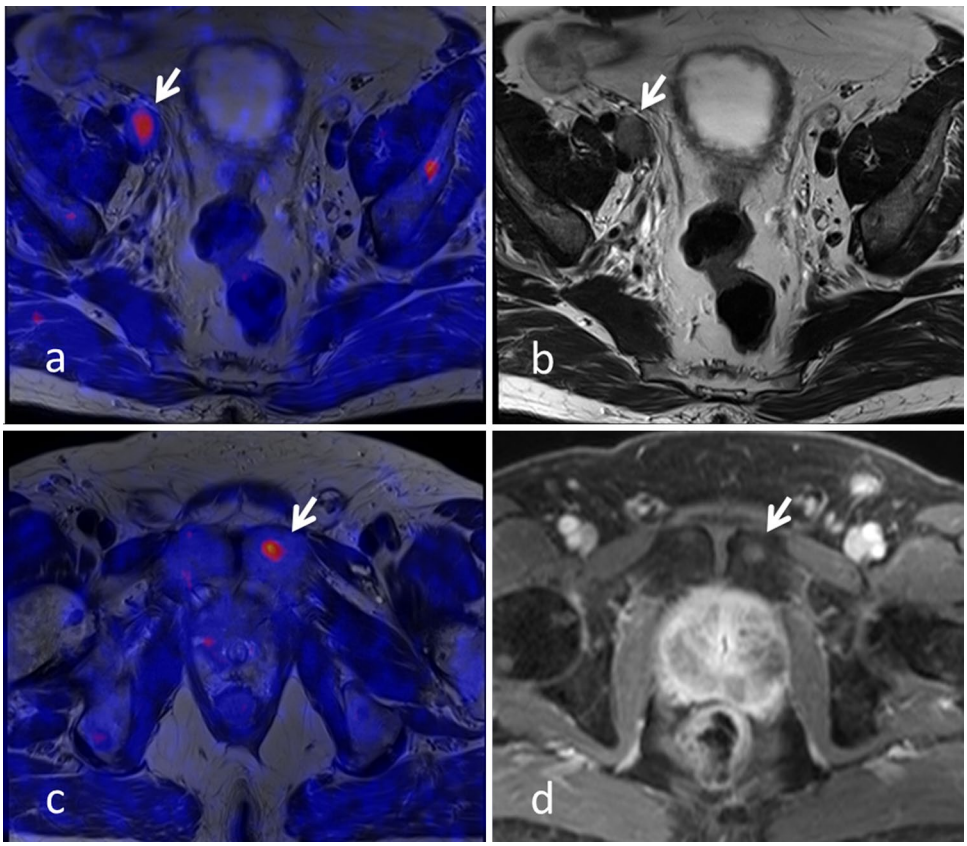

Fig. 4: 68-year-old patient with a histologically proven high-risk PC in the right peripheral zone (Gleason 9) and a PSA level of 14.5 ng/mL. Fused PET/MRI (^{11}C-choline) transversal image as well as conventional MR images showed local lymph-node metastasis (**a**, **b**; arrow) and bone metastasis (**c**, **d**; arrow)

assessment of local tumor extend. We found no significant differences between ^{11}C-choline and ^{68}Ga-PSMA-11 for local tumor detection. In comparison to the pathohistological gold standard, mpMRI showed 100% agreement for primary tumor extent, whereas PET with ^{11}C-choline as well as with ^{68}Ga-PSMA-11 both underestimated the local tumor extent. Using PET for seminal vesicle invasion is not feasible, whereas mpMRI detected seminal vesicle invasion in all cases. PET using ^{11}C-choline for diagnosis of primary prostate cancer have been examined in numerous trials with conflicting results, especially with respect to the sensitivity reported for the detection of primary prostate cancer showing a large variation between 60 and 100% studies. The first published study on ^{68}Ga-PSMA-11-PET/MRI for local extension of primary PC by Eiber et al. described a good correlation between findings from mpMRI and PSMA-PET, for localization of PC in patients selected for RP [20]. We also found correlations between findings from mpMRI and PET, but we did not find an additional value of PET for local staging. In line with our results, Giesel et al. presented a retrospective study with ten patients with primary PC, who underwent mpMRI and PSMA-PET/CT for initial staging. They concluded that PSMA-PET/CT and mpMRI correlated well with regard to tumor localization in these patients [14]. A major limitation of this retrospective analysis was that patients underwent radiotherapy, so that no histopathology comparison was available [14]. Rahbar et al. performed ^{68}Ga-PSMA-PET/CT in 6 patients with high-risk prostate cancer before radical prostatectomy and concluded that the intraprostatic localization and extent of prostate cancer may be estimated by ^{68}Ga-PSMA-11-PET, but they did not compare local staging with mpMRI as gold standard [21]. Fendler et al. evaluated the local staging of PC with ^{68}Ga-PSMA-11-PET/CT and concluded that ^{68}Ga-PSMA-11-PET/CT was able to accurately detect the location and extent of primary prostate cancer as well as seminal vesicle invasion with an 86% accuracy, and extracapsular extension with a 71% accuracy, respectively [22]. We observed a relevant difference concerning the extraprostatic extension with seminal vesicle invasion, which was missed in all patients by PET but correctly classified by mpMRI. The combination of mpMRI and PET should also be restricted to intermediate to high-risk PC, based on the previous study by Afshar-Oromieh et al., who described that prostate cancer patients with a Gleason score >7 or PSA levels ≥ 10 ng/mL showed a significantly higher uptake of ^{68}Ga-PSMA-11-PET than prostate cancer patients with lower Gleason scores [23]. In our series, ^{11}C-choline was not inferior compared to ^{68}Ga-PSMA-11-PET. One of the possible reasons for the non-inferiority could be that choline PET detects hrPC more readily as shown by Piert et al. [24]. In a study by Park et al., who compared ^{11}C-choline PET with whole-mount histology, a good delineation of local disease was also found [25]. It is well known that CT and MRI, with a pooled sensitivity of 42% and 39%, and a pooled specificity of 82% for both modalities, appear to be insufficient to reliably detect lymph-node metastases [10]. The sensitivity of ^{68}Ga-PSMA-11-PET as well as ^{11}C-choline PET for lymph-node involvement in various studies varied between 33.3 and 94% [26]. Concerning the diagnostic performance for identification of LNM in our study, PET/MRI scans identified 2 of 5 patients with OND, who underwent RP (1 in ^{68}Ga-PSMA-11-PET; 1 in ^{11}C-choline PET) as LN positive (true positive) with overall 662 resected LNs of which 9 harbored metastases (1%) in 5 of 24 patients (21%).

In studies about the assessment of LNM in biochemical recurrence of PC, PSMA-PET shows promising results. Rauscher et al. reported on ^{68}Ga-PSMA-11-PET-positive LNM in 53/68 (77.9%), which were pathologically confirmed as metastatic lymph nodes, while morphological imaging with CT was positive in only 18/67 cases (26.9%) [27]. Concerning sensitivity and specificity of ^{68}Ga-PSMA-11-PET imaging for lymph-node staging in primary PC, only a few articles reported histopathologic correlation [21, 26, 28]. Budaus et al. reported a histological confirmed analysis of patients with high-risk PC and concluded that LNM detection rates were substantially influenced by lymph-node metastasis size [26]. In line with our results, they also described an overall sensitivity of ^{68}Ga-PSMA-11-PET/CT for LNM detection of 33.3%, and a specificity of 100%. In contrast to our results as well as in contrast to Budaus et al., Herlemann et al. performed ^{68}Ga-PSMA-11-PET/CT prior to lymph-node dissection, and described an overall sensitivity and specificity of ^{68}Ga-PSMA-11-PET/CT for LNM detection of 84% and 82% [29], but lymphadenectomy was not restricted to OND. Van Leeuwen et al. also reported in a prospective study with 30 patients with intermediate- or high-risk PC undergoing preoperative ^{68}Ga-PSMA-11-PET/CT, that ^{68}Ga-PSMA-11-PET/CT had a high specificity, but a moderate sensitivity of 64% for LNM detection [30]. Among the largest cohort with primary staging including 130 patients with high-risk prostate cancer before radical prostatectomy, Maurer et al. described a similar sensitivity of 66%, while specificity was as high as 99% [28]. The value of ^{11}C-choline PET for lymph-node staging was described as limited [31] which also holds true for detection of every single LNM with ^{68}Ga-PSMA-11-PET.

In summary, the published data as well as our study revealed that hybrid imaging with ^{68}Ga-PSMA-11 is limited in detecting all small LNMs prior to RP when using histology as the reference standard.

The present study is not devoid of limitations. First, no randomization was performed. The cohort was small due to strict inclusion criteria and one-third of high-risk patients

did not undergo a surgical treatment due to metastatic disease. However, to date, most studies that reported about mpMRI and hybrid imaging correlation or co-registration had limited patient sample sizes [32, 33]. Finally, we did not consider costs of procedures. Regarding our results and the current literature, the combination of PET-CT for N- and M-staging with an additional mpMRI for T-staging appears more cost-effective and is more widely available. Therefore, this combination might be suitable in most cases. Combined PET/MRI, however, allows for direct imaging fusion which might be beneficial in specific cases.

Conclusions

In this prospective comparative study, we provide evidence for high diagnostic accuracy of mpMRI for the detection of primary PC localization and tumor extent. We observed no additional value for PET imaging concerning the primary tumor extend. We found no relevant differences between ^{68}Ga-PSMA-11 and ^{11}C-choline with respect to whole-body staging in the high-risk cohort. Importantly, wbPET/MRI is limited in detecting small LNMs prior to RP, independent of the tracer used. Despite the promising advances in PSMA-based imaging in the setting of biochemical recurrence, there is a need for further prospective, multi-center studies before integrating PET imaging into primary staging. Nonetheless, PSMA-PET can still be considered one of the most promising approaches for PC imaging based on its unique and stable expression in PC cells.

Author contributions SK: protocol/project development; data collection or management; data analysis; manuscript writing/editing; statistical analysis. SK: protocol/project development; data collection or management; data analysis; manuscript writing/editing. SG: protocol/project development; data collection or management; data analysis; manuscript writing/editing; statistical analysis. TH: data analysis; manuscript writing/editing; statistical analysis. WMT: data analysis; manuscript writing/editing; statistical analysis. JH: data collection or management; manuscript writing/editing. JS: data analysis; manuscript writing/editing. MS: data collection or management; manuscript writing/editing. KN: data analysis; manuscript writing/editing; administrative, technical, or material support; supervision. AS: manuscript writing/editing; supervision. GR: protocol/project development; manuscript writing/editing; administrative, technical, or material support. CF: data analysis; manuscript writing/editing; administrative, technical, or material support; supervision. JB: protocol/project development; data analysis; manuscript writing/editing.

Funding No funding was received for this work.

Compliance with ethical standards

Conflict of interest All authors declare that they have no conflict of interest.

Ethical approval All procedures performed in this study were in accordance with the ethical standards of the institutional research committee, approved by the local institutional review board (241/2012MPG23), and in line with the 1964 Helsinki declaration and its later amendments.

Informed consent Informed consent was obtained from all individual participants included in the study.

References

1. Torre LA, Bray F, Siegel RL, Ferlay J, Lortet-Tieulent J (2012) Jemal A (2015) Global cancer statistics. CA Cancer J Clin 65(2):87–108. https://doi.org/10.3322/caac.21262
2. Siegel RL, Miller KD (2016) Jemal A (2016) Cancer statistics. CA Cancer J Clin 66(1):7–30. https://doi.org/10.3322/caac.21332
3. Cooperberg MR, Cowan J, Broering JM, Carroll PR (2008) High-risk prostate cancer in the United States, 1990–2007. World J Urol 26(3):211–218. https://doi.org/10.1007/s00345-008-0250-7
4. D'Amico AV, Whittington R, Malkowicz SB, Schultz D, Blank K, Broderick GA, Tomaszewski JE, Renshaw AA, Kaplan I, Beard CJ, Wein A (1998) Biochemical outcome after radical prostatectomy, external beam radiation therapy, or interstitial radiation therapy for clinically localized prostate cancer. JAMA 280(11):969–974
5. Oesterling JE (1993) Using PSA to eliminate the staging radionuclide bone scan. Significant economic implications. Urol Clin N Am 20(4):705–711
6. Briganti A, Blute ML, Eastham JH, Graefen M, Heidenreich A, Karnes JR, Montorsi F, Studer UE (2009) Pelvic lymph node dissection in prostate cancer. Eur Urol 55(6):1251–1265. https://doi.org/10.1016/j.eururo.2009.03.012
7. Checcucci E, Amparore D, De Luca S, Autorino R, Fiori C, Porpiglia F (2019) Precision prostate cancer surgery: an overview of new technologies and techniques. Minerva Urol Nefrol 71(5):487–501. https://doi.org/10.23736/s0393-2249.19.03365-4
8. Jazayeri SB, Weissman B, Samadi DB (2018) Outcomes following robotic-assisted laparoscopic prostatectomy: Pentafecta and Trifecta achievements. Minerva Urol Nefrol 70(1):66–73. https://doi.org/10.23736/s0393-2249.17.02909-5
9. Mottet N, Bellmunt J, Bolla M, Briers E, Cumberbatch MG, De Santis M, Fossati N, Gross T, Henry AM, Joniau S, Lam TB, Mason MD, Matveev VB, Moldovan PC, van den Bergh RCN, Van den Broeck T, van der Poel HG, van der Kwast TH, Rouviere O, Schoots IG, Wiegel T, Cornford P (2017) EAU-ESTRO-SIOG guidelines on prostate cancer. Part 1: screening, diagnosis, and local treatment with curative intent. Eur Urol 71(4):618–629. https://doi.org/10.1016/j.eururo.2016.08.003
10. Hovels AM, Heesakkers RA, Adang EM, Jager GJ, Strum S, Hoogeveen YL, Severens JL, Barentsz JO (2008) The diagnostic accuracy of CT and MRI in the staging of pelvic lymph nodes in patients with prostate cancer: a meta-analysis. Clin Radiol 63(4):387–395. https://doi.org/10.1016/j.crad.2007.05.022
11. Albisinni S, Aoun F, Marcelis Q, Jungels C, Al-Hajj Obeid W, Zanaty M, Tubaro A, Roumeguere T, De Nunzio C (2018) Innovations in imaging modalities for recurrent and metastatic prostate cancer: a systematic review. Minerva Urol Nefrol 70(4):347–360. https://doi.org/10.23736/s0393-2249.18.03059-x
12. Rosenkrantz AB, Friedman K, Chandarana H, Melsaether A, Moy L, Ding YS, Jhaveri K, Beltran L, Jain R (2016) Current status of hybrid PET/MRI in oncologic imaging. AJR Am J Roentgenol 206(1):162–172. https://doi.org/10.2214/AJR.15.14968
13. Afshar-Oromieh A, Zechmann CM, Malcher A, Eder M, Eisenhut M, Linhart HG, Holland-Letz T, Hadaschik BA, Giesel FL, Debus

J, Haberkorn U (2014) Comparison of PET imaging with a (68)Ga-labelled PSMA ligand and (18)F-choline-based PET/CT for the diagnosis of recurrent prostate cancer. Eur J Nucl Med Mol Imaging 41(1):11–20. https://doi.org/10.1007/s00259-013-2525-5

14. Giesel FL, Sterzing F, Schlemmer HP, Holland-Letz T, Mier W, Rius M, Afshar-Oromieh A, Kopka K, Debus J, Haberkorn U, Kratochwil C (2016) Intra-individual comparison of (68)Ga-PSMA-11-PET/CT and multi-parametric MR for imaging of primary prostate cancer. Eur J Nucl Med Mol Imaging 43(8):1400–1406. https://doi.org/10.1007/s00259-016-3346-0
15. Schwenck J, Rempp H, Reischl G, Kruck S, Stenzl A, Nikolaou K, Pfannenberg C, la Fougere C (2017) Comparison of (68)Ga-labelled PSMA-11 and (11)C-choline in the detection of prostate cancer metastases by PET/CT. Eur J Nucl Med Mol Imaging 44(1):92–101. https://doi.org/10.1007/s00259-016-3490-6
16. Eissa A, Elsherbiny A, Coelho RF, Rassweiler J, Davis JW, Porpiglia F, Patel VR, Prandini N, Micali S, Sighinolfi MC, Puliatti S, Rocco B, Bianchi G (2018) The role of 68Ga-PSMA PET/CT scan in biochemical recurrence after primary treatment for prostate cancer: a systematic review of the literature. Minerva Urol Nefrol 70(5):462–478. https://doi.org/10.23736/s0393-2249.18.03081-3
17. Evangelista L, Guttilla A, Zattoni F, Muzzio PC, Zattoni F (2013) Utility of choline positron emission tomography/computed tomography for lymph node involvement identification in intermediate- to high-risk prostate cancer: a systematic literature review and meta-analysis. Eur Urol 63(6):1040–1048. https://doi.org/10.1016/j.eururo.2012.09.039
18. Weinreb JC, Barentsz JO, Choyke PL, Cornud F, Haider MA, Macura KJ, Margolis D, Schnall MD, Shtern F, Tempany CM, Thoeny HC, Verma S (2016) PI-RADS prostate imaging—reporting and data system: 2015, version 2. Eur Urol 69(1):16–40. https://doi.org/10.1016/j.eururo.2015.08.052
19. Sobin LH, Gospodariwicz M, Wittekind C (2009) TNM classification of malignant tumors UICC International Union Against Cancer, vol 7. Wiley-Blackwell, New York, pp 243–248
20. Eiber M, Weirich G, Holzapfel K, Souvatzoglou M, Haller B, Rauscher I, Beer AJ, Wester HJ, Gschwend J, Schwaiger M, Maurer T (2016) Simultaneous (68)Ga-PSMA HBED-CC PET/MRI improves the localization of primary prostate cancer. Eur Urol 70(5):829–836. https://doi.org/10.1016/j.eururo.2015.12.053
21. Rahbar K, Weckesser M, Huss S, Semjonow A, Breyholz HJ, Schrader AJ, Schafers M, Bogemann M (2016) Correlation of intraprostatic tumor extent with (6)(8)Ga-PSMA distribution in patients with prostate cancer. J Nucl Med 57(4):563–567. https://doi.org/10.2967/jnumed.115.169243
22. Fendler WP, Schmidt DF, Wenter V, Thierfelder KM, Zach C, Stief C, Bartenstein P, Kirchner T, Gildehaus FJ, Gratzke C, Faber C (2016) ^{68}Ga-PSMA PET/CT detects the location and extent of primary prostate cancer. J Nucl Med 57(11):1720–1725. https://doi.org/10.2967/jnumed.116.172627
23. Afshar-Oromieh A, Malcher A, Eder M, Eisenhut M, Linhart HG, Hadaschik BA, Holland-Letz T, Giesel FL, Kratochwil C, Haufe S, Haberkorn U, Zechmann CM (2013) PET imaging with a [^{68}Ga]gallium-labelled PSMA ligand for the diagnosis of prostate cancer: biodistribution in humans and first evaluation of tumour lesions. Eur J Nucl Med Mol Imaging 40(4):486–495. https://doi.org/10.1007/s00259-012-2298-2
24. Piert M, Park H, Khan A, Siddiqui J, Hussain H, Chenevert T, Wood D, Johnson T, Shah RB, Meyer C (2009) Detection of aggressive primary prostate cancer with ^{11}C-choline PET/CT using multimodality fusion techniques. J Nucl Med 50(10):1585–1593. https://doi.org/10.2967/jnumed.109.063396
25. Park H, Meyer CR, Wood D, Khan A, Shah R, Hussain H, Siddiqui J, Seo J, Chenevert T, Piert M (2010) Validation of automatic target volume definition as demonstrated for ^{11}C-choline PET/CT of human prostate cancer using multi-modality fusion techniques. Acad Radiol 17(5):614–623. https://doi.org/10.1016/j.acra.2010.01.003
26. Budaus L, Leyh-Bannurah SR, Salomon G, Michl U, Heinzer H, Huland H, Graefen M, Steuber T, Rosenbaum C (2016) Initial experience of (68)Ga-PSMA PET/CT imaging in high-risk prostate cancer patients prior to radical prostatectomy. Eur Urol 69(3):393–396. https://doi.org/10.1016/j.eururo.2015.06.010
27. Rauscher I, Maurer T, Beer AJ, Graner FP, Haller B, Weirich G, Doherty A, Gschwend JE, Schwaiger M, Eiber M (2016) Value of ^{68}Ga-PSMA HBED-CC PET for the assessment of lymph node metastases in prostate cancer patients with biochemical recurrence: comparison with histopathology after salvage lymphadenectomy. J Nucl Med 57(11):1713–1719. https://doi.org/10.2967/jnumed.116.173492
28. Maurer T, Gschwend JE, Rauscher I, Souvatzoglou M, Haller B, Weirich G, Wester HJ, Heck M, Kubler H, Beer AJ, Schwaiger M, Eiber M (2016) Diagnostic efficacy of (68)Gallium-PSMA positron emission tomography compared to conventional imaging for lymph node staging of 130 consecutive patients with intermediate to high risk prostate cancer. J Urol 195(5):1436–1443. https://doi.org/10.1016/j.juro.2015.12.025
29. Herlemann A, Wenter V, Kretschmer A, Thierfelder KM, Bartenstein P, Faber C, Gildehaus FJ, Stief CG, Gratzke C, Fendler WP (2016) (68)Ga-PSMA positron emission tomography/computed tomography provides accurate staging of lymph node regions prior to lymph node dissection in patients with prostate cancer. Eur Urol 70(4):553–557. https://doi.org/10.1016/j.eururo.2015.12.051
30. van Leeuwen PJ, Emmett L, Ho B, Delprado W, Ting F, Nguyen Q, Stricker PD (2017) Prospective evaluation of ^{68}Gallium-prostate-specific membrane antigen positron emission tomography/computed tomography for preoperative lymph node staging in prostate cancer. BJU Int 119(2):209–215. https://doi.org/10.1111/bju.13540
31. Hacker A, Jeschke S, Leeb K, Prammer K, Ziegerhofer J, Sega W, Langsteger W, Janetschek G (2006) Detection of pelvic lymph node metastases in patients with clinically localized prostate cancer: comparison of [^{18}F]fluorocholine positron emission tomography-computerized tomography and laparoscopic radioisotope guided sentinel lymph node dissection. J Urol 176(5):2014–2019. https://doi.org/10.1016/j.juro.2006.07.037
32. Rhee H, Thomas P, Shepherd B, Gustafson S, Vela I, Russell PJ, Nelson C, Chung E, Wood G, Malone G, Wood S, Heathcote P (2016) Prostate specific membrane antigen positron emission tomography may improve the diagnostic accuracy of multiparametric magnetic resonance imaging in localized prostate cancer. J Urol 196(4):1261–1267. https://doi.org/10.1016/j.juro.2016.02.3000
33. Zamboglou C, Drendel V, Jilg CA, Rischke HC, Beck TI, Schultze-Seemann W, Krauss T, Mix M, Schiller F, Wetterauer U, Werner M, Langer M, Bock M, Meyer PT, Grosu AL (2017) Comparison of (68)Ga-HBED-CC PSMA-PET/CT and multiparametric MRI for gross tumour volume detection in patients with primary prostate cancer based on slice by slice comparison with histopathology. Theranostics 7(1):228–237. https://doi.org/10.7150/thno.16638